# Accepted Manuscript

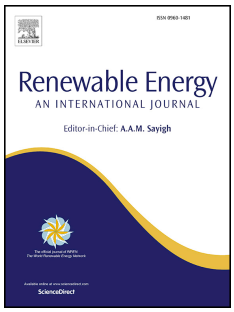


Optimization of microwave-assisted biodiesel production from Papaya oil using response surface methodology

Milap G. Nayak, Amish P. Vyas

PII: S0960-1481(19)30054-0

DOI: https://doi.org/10.1016/j.renene.2019.01.054

Reference: RENE 11055

To appear in: *Renewable Energy*

Received Date: 24 March 2018

Revised Date: 8 October 2018

Accepted Date: 14 January 2019

Please cite this article as: Nayak MG, Vyas AP, Optimization of microwave-assisted biodiesel production from Papaya oil using response surface methodology, *Renewable Energy* (2019), doi: https://doi.org/10.1016/j.renene.2019.01.054.

# Optimization of microwave-assisted biodiesel production from Papaya oil using response surface methodology

Milap G. Nayak[1]*, Amish P. Vyas[2]

[1]Chemical Engineering Department, V.G.E.C.-Chandkheda, Gujarat Technological University, Ahmedabad-382424, Gujarat, India

[2]Saffrony Institute of Technology, At & P.-Linch, Mehsana – 384435, Gujarat Technological University, Gujarat, India

***Abstract***

In these studies, the microwave-assisted transesterification of non-edible Papaya oil was investigated under the fixed microwave power of 700 W and constant magnetic stirring. Optimization of the yield of Papaya oil methyl ester was investigated using response surface methodology. Within the range of the selected operating conditions, the optimized values of temperature, catalyst amount, time, and methanol to oil molar ratio were found to be 62.33 °C, 0.95 wt %, 3.30 minutes, and 9.50:1 respectively. Current studies revealed that the methanol to oil molar ratio and temperature have significant effects on microwave-assisted transesterification of Papaya oil. The high values of $R^2$ 97.72 and $R^2_{adj}$ 95.60 indicate that the fitted model shows a good agreement with the predicted and actual FAME yield. Based on the optimum condition, the predicted biodiesel yield was 99.9% and the actual experimental value was 99.3%. Papaya oil methyl ester (POME) exhibits property close to ASTM standards. In conclusion, these studies revealed that biodiesel obtained from Papaya seed oil feedstock has a potential to use as an alternative of diesel.

*Keywords*

Response Surface Methodology (RSM)
Central Composite Design
Papaya oil methyl ester (POME)
Transesterification
Microwave
Biodiesel

## 1. Introduction

Conventional energy sources like coal and petroleum crude are polluting and depleting rapidly due to high energy demand. The rapid rise in population, as well as industrial and technological developments trigger energy crisis[1]. Moreover, increasing awareness towards environmental concerns, stringent emission norms, and fluctuating prices of the crude oil encourage society to use renewable energy sources[2]. The International energy agency reported biofuel as the highly sustainable energy among wind, solar and hydro energy sources[3,4]. Biodiesel, commonly known as the ester of fatty acid synthesized by esterification of free fatty acid(FFA) and trans-esterification of triacylglycerides with reacting species like alcohols[5]. The inter-esterification of oil with short-chain esters, acetates[6–8] and alkyl carbonates[9,10] have also been reported. Biodiesel has gained more importance over the past two decades due to its renewability, biodegradability, and non-toxic nature[11]. It has high calorific value, cetane number, flash point, low sulfur and aromatics contents compared to diesel. Moreover, it can directly run the diesel engine without compromising the engine performance[12–14]. Vegetable oilseeds including soybean, canola, palm kernel, sunflower, and coconut were explored as feedstock for biodiesel production but constrained by food security and serious ecological imbalance due to the destruction of forest for large-scale plantation of edible crops [14–16]. As a result, various non-edible oil bearing seeds such as C. pentandra[17], Neem[18], Mahua [19], Karanja [18], Jathropha[20] were explored for biodiesel production. Availability and the cost of feedstock strongly influenced the over all cost of biodiesel. India is one of the largest Papaya producing country followed by Brazil, Indonesia, the Dominican Republic, Nigeria, and Mexico. Production of Papaya was 56,39,300 tons per annum with harvested area of 42.28 T/ha in India which contributed to 35% of the world's Papaya production[21,22]. Out of 1kg Papaya, 300 g of waste is produced including 160 g of seeds. The oil content of Papaya seed varied from 15.3 to 30%. Hence, worldwide Papaya oil production is approximate 3,20,470 Tons/annum[23].In the literature, transesterification of edible and non-edible oils were explored using homogeneous and heterogeneous catalysts involving conventional heating[3,14,24–

29], enzyme catalytic[30], supercritical [31–35], ultrasound [36–39] and microwave heating[40–44].Out of these, microwave supported trans-esterification reaction is rapid and less energy intensive.. Therefore, microwave-assisted transesterification of Papaya seed oil has explored in these studies. There are numerous parameters those affects the yield of biodiesel under microwave-assisted trans-esterification of vegetable oils. Under fixed microwave power and agitation speed, these are alcohol to oil molar ratio, catalyst concentration, reaction temperature, and reaction time. Influence of individual parameter and their interactions can't be generalized and it is a key challenge in the optimization of process parameters to achieve maximum biodiesel yield. It requires a large number of experiments, therefore, statistical techniques such as response surface methodology was applied for microwave-assisted optimization of biodiesel from Papaya oil. So far, two-step production of Carica Papaya oil methyl ester has been reported in the literature. The process parameters were: 2 wt% $H_2SO_4$, 9:1 molar ratio, 100°C temperature and 2h reaction time[45]. However, to the best of our knowledge, optimization of microwave-assisted transesterification of Papaya seed oil to produce biodiesel, using response surface methodology has not yet described in the literature. In these studies, optimizations of trans-esterification process parameters' are carried out using response surface methodology in combination with the central composite design.

Abbreviation

PO Papaya Oil
POME Papaya Oil Methyl Ester
FFA Free Fatty Acid
RSM Response Surface Methodology
CCD Central Composite Design

## 2. *Materials and methods*

Refined Papaya oil (PO) was purchased from M/s Katyani Exports Pvt Ltd, New Delhi. The All chemicals such as NaOH, KOH, methanol, and ethanol were analytical reagent grade. **Table 1** presents physicochemical properties and fatty acid composition derived from GC-MS (supplementary S1) of Papaya oil. The observed FFA content of PO was 1.6%. It was less than 2%, therefore, pre-treatment or esterification with acid catalyst could be avoided, and homogenous alkali catalyst NaOH used directly for the transesterification reaction. The mean molecular weight of Papaya oil based on fatty acid composition was calculated by Eq (1),

3*(Average MW of FFA) + MW of glycerol – 3* MW of water (1)

=3*(276) + 92 – 3*54

=866 g/mol

The molecular weight of oil calculated from saponification and acid value of oil using formula MW =168300/(SV- AV) was found to be 871 g/mol.

Table 1
Physicochemical properties and characteristic of Papaya oil

| Properties(unit) | **Papaya oil** |
|---|---|
| Specific gravity($gcc^{-1}$) | 0.907 |
| Viscosity at 40 °C (cSt) $mm^2s^{-1}$ | 29.30 |
| Saponification number (mg $g^{-1}$) | 194 |
| Iodine number | 76 |
| Free fatty acids% | 1.60 |
| Acid number (mg KOH $g^{-1}$) | 0.80 |
| Fatty acid composition | (wt%) |
| Myristic acid C14:1 | 0.21 |
| Palmitic acid C16:0 | 9.33 |
| Palmitoleic acid C16:1 | 0.73 |
| Oleic acid c18:1 | 80.57 |
| Linoleic acid C18:2 | 0.71 |
| Arachidic acid C20:0 | 1.17 |
| Eicosenoic acid C20:1 | 1.46 |
| Behenic acid C22:0 | 1.96 |
| Lignoceric acid C24:0 | 0.99 |
| Saturated fatty acid | 13.66 |
| Monounsaturated fatty acid | 82.69 |
| Polyunsaturated fatty acid | 0.71 |
| Degree of unsaturation | 84.11 |
| Mean molecular weight($gmol^{-1}$) | 866-871 |

**Table 1: Physicochemical properties and fatty acid composition of Papaya oil**

## *3. Experimental design*

### *3.1 Experimental set up*

The batch experiments were carried out in a 100 mL single neck reaction flask (reactor) containing Papaya oil, methanol, and sodium hydroxide catalyst. As presented in **Figure 1**, commercial Raga's microwave reactor was used for experimentation. It has an internal volume of 31 litre, operating at 2450 GHz with a maximum power output of 700 W. The temperature of the reactor was measured with an infrared temperature sensor. The glass reactor connected to a reflux condenser. Due to rapid heating by microwave, methanol get vaproized hence, chilled water was supplied for condensation to ensure the retention of methanol into the reactor. The reaction mixture was subjected to irradiation under 700 W microwave power output and constant magnetic stirring for all the experiments**.**

Figure 1
Microwave reactor for transesterification reaction


**Figure 1: Microwave-assisted transesterification of Papaya oil using methanol and alkali catalyst**

### *3.2 Microwave-assisted transesterification*

Microwaves (MW) are non-ionizing electromagnetic waves having a wavelength between 1 mm and 1 m depending on the frequencies varying from 0.3 and 300 GHz [46]. The heat generation observed during reaction mainly due to high-frequency rotation of alcohol under rapidly changing electric and magnetic field commonly known as dipole rotation. Also, ions present in the solution oscillate, slow down and change its direction under applied varying electric field generates heat by conduction. These two phenomena termed as dielectric heating[47]. Methanol is a polar molecule with a high dielectric constant is preferred for microwave assisted trans-esterification reaction. Microwave-assisted transesterification of Papaya oil was carried out with a varying quantity of methanol, catalyst concentration, temperature, and time. At the end of the reaction, samples were cooled and kept in separating funnel. Biodiesel phase separated at the top due to its low density than heavier glycerol phase. The top layer of biodiesel was removed, heated above 65°C to remove traces of alcohol and washed with distilled water to remove traces of NaOH. Samples were dried and passed through anhydrous $Na_2SO_4$ to

remove traces of water. The purity of biodiesel was checked using the method described in 3:27 test[48]. The yield of biodiesel was determined using Eq (2).

$$\text{Yield of biodiesel} = (A/B) * 100 \quad (2)$$

Where,

A: Amount of biodiesel produced, g

B: Theoretical maximum amount of biodiesel produced, g.

### *3.3 Statistical analysis*

The response surface methodology (RSM) in conjunction with central composite design (CCD) was used to design the experiments, model and to optimize POME yield as the response for microwave-assisted base-catalyzed transesterification process. The CCD was a suitable design for sequential experiments to obtain appropriate information for testing lack of fit without a large number of design points[49]. In this study, four independent variables temperature °C ($X_1$), catalyst amount ($X_2$), time ($X_3$), and the molar ratio of methanol to oil ($X_4$) coded into three levels. The axial points distance from the center coded as −2 (−α) and +2 (+α) and presented in **Table 2**.

Table 2
Variables presented in coded form

| Variables | Symbol | Level | | | | |
|---|---|---|---|---|---|---|
| | | α= -2 | -1 | 0 | 1 | α = 2 |
| Temperature, °C | $X_1$ | 50 | 55 | 60 | 65 | 70 |
| Catalyst wt% | $X_2$ | 0.5 | 0.75 | 1 | 1.25 | 1.5 |
| Time, minute | $X_3$ | 0.5 | 3 | 5.5 | 8 | 10.5 |
| Molar ratio | $X_4$ | 3:1 | 6:1 | 9:1 | 12:1 | 15:1 |

Transformation of variable levels from coded (X) to uncoded was obtained as: $X_1= 5X+60$ ,$X_2= 0.25X +1$, $X_3= 2.5X+5.5$ , $X_4 = 3X+9$

**Table 2 : RSM experimental design for four variables at three levels showing coded and uncoded values**

The Minitab 16 software was used for regression, graphical analysis, statistical analysis, and optimization of POME yield. It required 30 experiments according to $2^k+2k+ 6$, where k is the number of independent variables[50]. It included sixteen factorial, eight axial, and six replicates points at the

centre. The centre points repeated 4–6 times to determine the experimental error (pure error) and the reproducibility of the data. The complete CCD design matrix including real and coded independent variable is presented in **Table 3**. Experimental POME yield correlated with independent variables by second-order polynomial Eq (3).

$$Y = \beta 0 + \sum_{j=1}^{j=k} \beta jXj + \sum\sum_{i<j} \beta ijXiXj + \sum_{j=1}^{j=k} \beta jjXj2 + \varepsilon \quad (3)$$

Where,

Y: The response, POME yield

Xi, Xj: Independent variable

β0: intercept

βi: The first order coefficient of the model

βjj: The quadratic coefficient of j factor

βij: The linear coefficients of the model for the interaction between i and j factors

k: The number of factors studied and optimized in the experiment

ε: The experimental error attributed to Y.

The regression coefficient of determination or relative standard error (RSEE) observed between the experimental and predicted results indicated the criteria for reliability evaluation of the model. The RSEE calculated by the Eq. 4. The average RSEE less than 10% was preferable[51].

$$RSEE\ \% = \sum_{i=1}^{i=n} \frac{|Yexp - Ypre|}{Yexp} * \frac{100}{n} \quad (4)$$

Where,

$Y_{,exp}$: The values obtained from experiments

$Y_{pre:}$ The values obtained from the model

N: Number of experimental results

177 Coefficients of determination, $R^2$ determine the quality of fit for the model and the analysis of variance

178 (ANOVA) was checked by Fisher's test (F-test).

Table 3
RSM-CCD design to measure response of POME

| Sr. No | Point Type | Temperature, °C ($X_1$) | | Catalyst wt% ($X_2$) | | Time, minute ($X_3$) | | Molar ratio ($X_4$) | | POME yield (Y) | Yield (Y') predicted | RSEE % |
|---|---|---|---|---|---|---|---|---|---|---|---|---|
| | | U.C | C | U.C. | C. | U.C. | C. | U.C | C. | | | |
| 1 | Axial | 60 | 0 | 0.5 | -2 | 5.5 | 0 | 9 | 0 | 71.00 | 70.62 | 0.54 |
| 2 | Fact | 65 | 1 | 1.25 | 1 | 8 | 1 | 12 | 1 | 67.00 | 70.15 | 4.71 |
| 3 | Fact | 55 | -1 | 0.75 | -1 | 8 | 1 | 6 | -1 | 58.00 | 61.05 | 5.25 |
| 4 | Centre | 60 | 0 | 1 | 0 | 5.5 | 0 | 9 | 0 | 98.80 | 96.46 | 2.36 |
| 5 | Centre | 60 | 0 | 1 | 0 | 5.5 | 0 | 9 | 0 | 93.00 | 96.46 | 3.72 |
| 6 | Fact | 65 | 1 | 0.75 | -1 | 3 | -1 | 6 | -1 | 63.00 | 64.44 | 2.29 |
| 7 | Centre | 60 | 0 | 1 | 0 | 5.5 | 0 | 9 | 0 | 93.20 | 96.46 | 3.50 |
| 8 | Fact | 55 | -1 | 0.75 | -1 | 8 | 1 | 12 | 1 | 78.22 | 79.38 | 1.48 |
| 9 | Fact | 55 | -1 | 1.25 | 1 | 8 | 1 | 6 | -1 | 62.00 | 60.77 | 1.97 |
| 10 | Axial | 50 | -2 | 1 | 0 | 5.5 | 0 | 9 | 0 | 52.00 | 53.39 | 2.69 |
| 11 | Fact | 55 | -1 | 1.25 | 1 | 3 | -1 | 6 | -1 | 61.00 | 64.37 | 5.53 |
| 12 | Fact | 65 | 1 | 1.25 | 1 | 3 | -1 | 12 | 1 | 86.00 | 82.60 | 3.94 |
| 13 | Fact | 55 | -1 | 1.25 | 1 | 8 | 1 | 12 | 1 | 57.00 | 55.21 | 3.13 |
| 14 | Fact | 55 | -1 | 1.25 | 1 | 3 | -1 | 12 | 1 | 61.00 | 57.75 | 5.32 |
| 15 | Axial | 60 | 0 | 1 | 0 | 0.5 | -2 | 9 | 0 | 89.20 | 92.89 | 4.14 |
| 16 | Axial | 60 | 0 | 1.5 | 2 | 5.5 | 0 | 9 | 0 | 55.00 | 56.48 | 2.69 |
| 17 | Fact | 65 | 1 | 0.75 | -1 | 8 | 1 | 6 | -1 | 59.00 | 61.49 | 4.22 |
| 18 | Fact | 65 | 1 | 1.25 | 1 | 8 | 1 | 6 | -1 | 60.00 | 60.96 | 1.61 |
| 19 | Fact | 55 | -1 | 0.75 | -1 | 3 | -1 | 6 | -1 | 58.00 | 54.08 | 6.74 |
| 20 | Axial | 60 | 0 | 1 | 0 | 5.5 | 0 | 15 | 2 | 67.00 | 70.78 | 5.64 |
| 21 | Centre | 60 | 0 | 1 | 0 | 5.5 | 0 | 9 | 0 | 96.00 | 96.46 | 0.48 |
| 22 | Centre | 60 | 0 | 1 | 0 | 5.5 | 0 | 9 | 0 | 99.00 | 96.46 | 2.55 |
| 23 | Fact | 55 | -1 | 0.75 | -1 | 3 | -1 | 12 | 1 | 72.67 | 71.36 | 1.80 |
| 24 | Fact | 65 | 1 | 0.75 | -1 | 8 | 1 | 12 | 1 | 98.30 | 94.58 | 3.78 |
| 25 | Axial | 70 | 2 | 1 | 0 | 5.5 | 0 | 9 | 0 | 79.00 | 78.70 | 0.38 |
| 26 | Axial | 60 | 0 | 1 | 0 | 5.5 | 0 | 3 | -2 | 47.00 | 44.31 | 5.70 |
| 27 | Fact | 65 | 1 | 0.75 | -1 | 3 | -1 | 12 | 1 | 96.00 | 96.46 | 0.48 |
| 28 | Axial | 60 | 0 | 1 | 0 | 10.5 | 2 | 9 | 0 | 90.00 | 87.40 | 2.88 |
| 29 | Centre | 60 | 0 | 1 | 0 | 5.5 | 0 | 9 | 0 | 98.80 | 96.46 | 2.36 |
| 30 | Fact | 65 | 1 | 1.25 | 1 | 3 | -1 | 6 | -1 | 76.4a 0 | 74.48 | 2.51 |
| | | | | | | | | | | | Avg. RSEE | 3.14% |

U.C. Uncoded value, C. Coded value

179 **Table 3: Experimental and predicted POME yield using RSM central composite design**

## *4. Result and discussion*

### *4.1. Development of Regression model*

Linear, linear and square, two-factor interaction, and quadratic polynomial model equations were used to fit the response of the experiment. The quadratic model selected as the best model due to its highest order polynomial with high F value, lower P-value, and high $R^2$ as shown in **Table 4**.

Table 4
The sequential model sum of squares

| Source | Sum of squares | DF | Mean Square | F value | Prob>F | $R^2$ |
|---|---|---|---|---|---|---|
| Linear | 2355.66 | 4 | 588.92 | 2.47 | 0.071 | 28.34 |
| Linear+ Square | 7124.57 | 8 | 890.57 | 15.73 | 0.000 | 85.70 |
| Linear+ Interaction | 3355.45 | 10 | 333.55 | 1.29 | 0.305 | 40.36 |
| Interaction | 999.31 | 6 | 166.63 | 13.21 | 0.731 | ------ |
| Quadratic | 8124.36 | 14 | 580.31 | 46 | 0.000 | 97.72 |

**Table 4: Evaluation of models for best fit with experimental yield**

Response yield, Y analyzed by response surface design using quadratic equation is expressed by Eq. (5)

$$Y = 96.446 + 6.3253*X_1 - 3.5330*X_2 - 1.3728*X_3 + 6.6164*X_4 - 7.6042*X_1^2 - 8.2292*X_2^2 - 1.5792*X_3^2 - 9.7292*X_4^2 - 0.0629*X_1*X_2 - 2.4783*X_1*X_3 + 3.6879*X_1*X_4 - 2.6408*X_2*X_3 - 5.9746*X_4*X_2 + 0.2658*X_3*X_4 \quad (5)$$

The terms with positive sign indicate the synergistic effect that increases POME yield, whereas a negative sign indicate hostile effect. **Table 5** presents the result of a statistical analysis of variance (ANOVA). It determined the significance fitness of the quadratic model as well as the effect of individual terms and their interaction on the POME yield. The probability of error or p-value measured the significance of each regression coefficient. The quadratic model with F value 46 and p-value <0.0001 for the experimental data indicates that it is significant at 95% confidence level. The molar ratio($X_4$), temperature($X_1$), catalyst loading($X_2$), and time($X_3$) have a significant influence on POME yield due to their low P-values. The molar ratio with F value, 83.23 contributes 44.58% to the response. Other terms with reducing F-values

200 are temperature (76.11), catalyst amount (23.75), and time (3.59) contributing 40.7%, 12.72%, and 2%
201 respectively. A low value of the coefficient of the variation (CV, 4.71%), indicates a high degree of
202 precision and a good deal of reliability with the experimental values. Adjusted-$R^2$ with 0.9560 reveals
203 95.60% of variability with the predicted versus actual values for POME yield was explained by the
204 model. $R^2$ with 0.9772 indicates close agreement between the predicted and experimental values. The
205 lower difference between $R^2$ and Adjusted-$R^2$ implies that all significant terms are involved in the model.
206 The lack of fit test having p-value 0.257 greater than 0.01 suggested that lack of fit is not significant.. The
207 model satisfactorily fitted to the experimental data and accounted all the contribution in the regression
208 response relationship[49].
209

Table 5
Test of significance for every regression coefficients and ANOVA(POME synthesis)

| Source | Coefficient | Coefficient p-value | SS | DF | MS | F-value | P-Value |
|---|---|---|---|---|---|---|---|
| Model | | | 8124.36 | 14 | 580.31 | 46.00 | <0.0001 |
| | β0 (96.4667) | 0.000 | | | | | |
| Temperaure,$X_1$ | β1(6.3253) | 0.000 | 960.22 | 1 | 960.22 | 76.11 | <0.0001 |
| Catalyst %,$X_2$ | β2(-3.5330) | 0.000 | 299.58 | 1 | 299.58 | 23.75 | <0.0001 |
| Time,$X_3$ | β3(-1.3728) | 0.078 | 154.77 | 1 | 154.77 | 3.59 | 0.0078 |
| Molar Ratio,$X_4$ | β4(6.6164) | 0.000 | 1050.63 | 1 | 1050.63 | 83.23 | <0.0001 |
| $X_1^2$ | β11(-7.6042) | 0.000 | 850.22 | 1 | 1586.04 | 125.72 | <0.0001 |
| $X_2^2$ | β22(-8.2292) | 0.000 | 1321.34 | 1 | 1857.47 | 147.23 | <0.0001 |
| $X_3^2$ | β33(-1.5792) | 0.034 | 1.00 | 1 | 68.41 | 5.42 | 0.034 |
| $X_4^4$ | β44(-9.7292) | 0.000 | 2596.34 | 1 | 2596.34 | 205.80 | <0.0001 |
| $X_1X_2$ | β12(-0.0629) | 0.944 | 0.06 | 1 | 0.06 | 0.01 | 0.944 |
| $X_1X_3$ | β13(-2.4783) | 0.014 | 98.27 | 1 | 98.27 | 7.79 | 0.014 |
| $X_1X_4$ | β14(3.6879) | 0.001 | 217.61 | 1 | 217.61 | 17.25 | <0.0001 |
| $X_2X_3$ | β23(-2.6408) | 0.009 | 111.58 | 1 | 111.58 | 8.84 | 0.009 |
| $X_2X_4$ | β24(-5.9746) | 0.000 | 571.13 | 1 | 571.13 | 45.27 | <0.0001 |
| $X_3X_4$ | β34(0.2658) | 0.769 | 1.13 | 1 | 1.13 | 0.09 | 0.796 |
| Residual | | | 189.24 | 15 | 189.24 | 12.62 | |
| Lack of fit | | | 149.02 | 10 | 149.02 | 14.90 | 0.257 |
| Pure-error | | | 40.21 | 5 | 40.21 | 8.04 | |
| Std. Dev. | | | 3.552 | | $R^2$ | 97.72 | |
| Mean | | | 74.7 | | Adj –$R^2$ | 95.60 | |
| C.V. | | | 4.71 | | Predicted-$R^2$ | 88.98 | |

210 **Table 5: ANOVA and test of significance of every variable using ANOVA for microwave-assisted POME synthesis**

**Figure 2a** presents the actual POME yield Vs. predicted POME yield. For good agreement with actual value, the predicated POME yield must lie close to the Y=X line. The model estimated response close to the experimental data for the system in the range studied. **Figure 2b** presents a normal probability plot of the residuals. The errors distribute normally across a straight line and insignificant. The structureless plot of residuals versus predicted response in **Figure 2c** suggests the minimum value of residual for predicted data. Most of the standard residuals should lie in the interval of ±5.00. Any observation outside this interval renders an operational error in the experimental data or a potential error in the model[32]. Histogram plot of the frequency of residual against residual in **Figure 2d** lies close to zero residual value indicated the minimum deviation of response with experimental data.

Figure 2a
Predicted Vs. actual POME yield

Figure 2b
Normal probability plot of residual

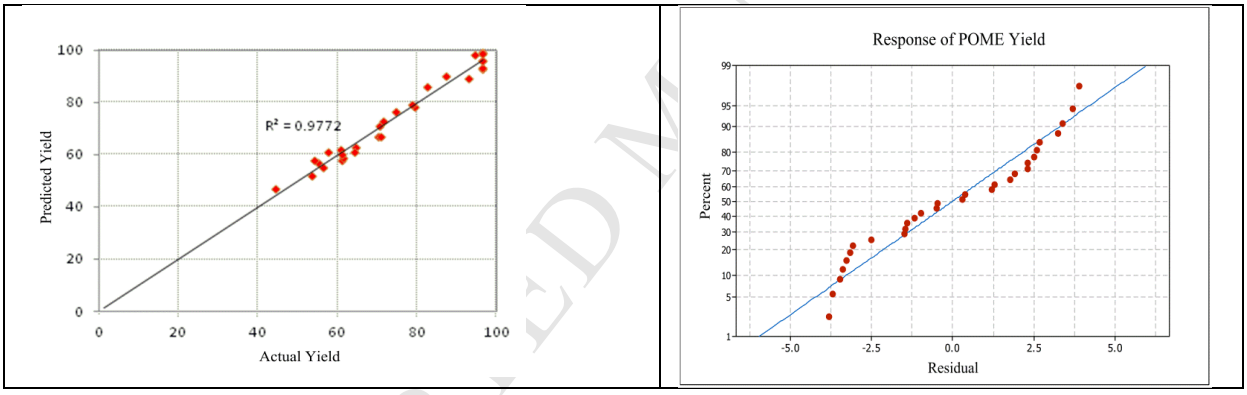


Figure 2c
Residual Vs. predicted response plot

Figure 2d
Histogram plot of frequency Vs. residual

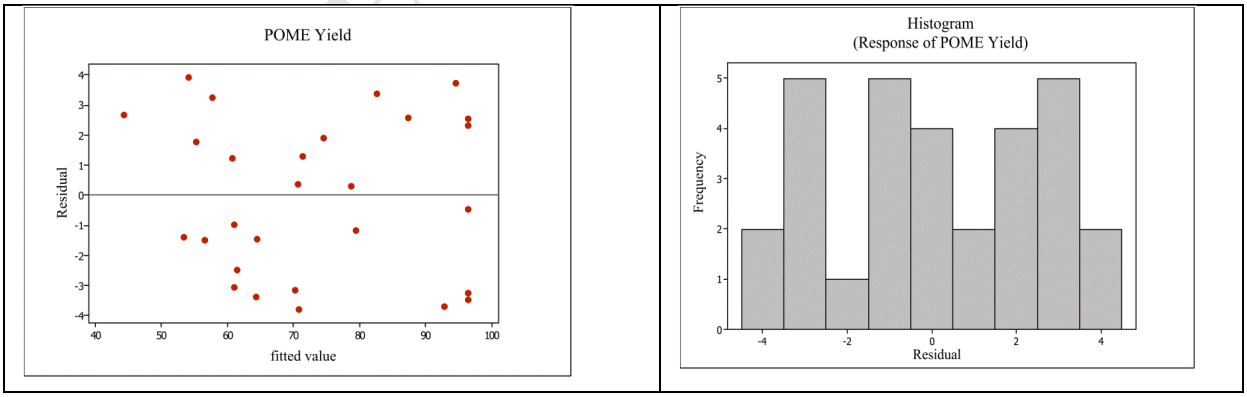


**Figure 2: Residual, histogram and predicted Vs. actual yield plots for POME synthesis**

### *4.2. Parameter study*

#### *4.2.1 Single parameter study*

**Figure 3** demonstrates the effect of individual variables on POME yield. The effect of the individual parameter on POME yield was determined by keeping other variables constant at hold value (0,0,0) in coded form. With increasing the temperature($X_1$) from 50°C to 62°C, the reaction yield increases. It is due to increase in reaction rate, reduction in oil viscosity, and improved solubility of oil with alcohol phase. However further increase in temperature from 62°C to 70°C resultes in a reduction of yield due to vaporization of methanol (Boiling point 64.5°C) and unfavourable saponification reaction over transesterification[49].

Figure 3

Effect of Individual variables on POME yield

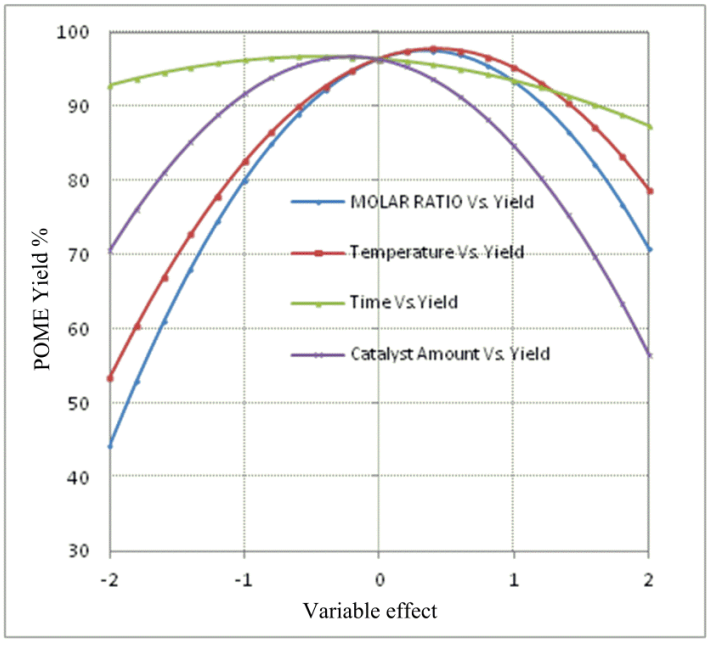


**Figure 3: Effect of individual variable on POME yield keeping other variables at hold values of zeros in coded form**

The catalyst improves the formation of methoxy radicals from methanol. The methoxy radicals combined with triglyceride to initiate the formation of biodiesel and glycerol. Hence, the yield increases from 70 % to 96.92% with increasing the catalyst concentration($X_2$) from 0.5wt% to 0.95 wt%. The addition of catalyst amount beyond 0.95 wt% reduces the POME yield from 96.92% to 56.25%. It is due to undesired soap formation reaction and increased in solution viscosity[49]. Soap formation reduces surface tension between biodiesel and glycerol phase, resulting in difficulty in separation and reduction in POME yield. Microwave-assisted transesterification yielded 96% POME within 1 minute. It is due to the high dielectric tangent of methanol as well as the complete solubility of NaOH catalyst in reaction mixture[52]. With the increase in a molar ratio from 3:1 to 10:1, reaction yield increases from 43 % to 97.62 %(127% increase). Hence, the higher molar ratio is preferred to increase the forward reaction rate. However, the POME yield decrease from 97.62% to 70% with a further increase in a molar ratio from 10:1 to 15:1, The decreasing trend observed mainly due to relative dilution of the catalyst, increasing the solubility of POME in glycerol phase and the reverse reaction rate[53].

### *4.2.2 Interaction of two parameter study*

The surface and contour plot used to establish the interactions between the parameters and their effect on POME yield. As the model has four variables, these plots were formed, each with two targeted variables, while the other two variables held constant at zeros in their coded values. The interaction of temperature($X_1$) and catalyst concentration($X_2$) on POME yield are presented in Figure 4a(3D surface plot) and Figure 4b(contour plot). Time and molar ratio kept at hold value of 5.5 minutes and 9:1 respectively. For all range of catalyst concentration under study, the increasing in temperature from 50 °C to 62 °C favours yield due to absorption of microwave energy by reaction mixture. However, the yield reduces when the temperature increases further from 62 °C to 70 °C. The main reason behind this is evaporation of methanol from the oil phase at a temperature above its boiling point[54]. Similarly, for a given temperature, increasing in catalyst amount from 0.5 wt% to 1 wt%, substantially improved the POME yield. However, it decreases at higher catalyst amount due to gel formation and increasing in

viscosity of the reaction mixture[55]. The yield enhances with an increasing in catalyst concentration and temperature but declines at excess level. The combined effect of high temperature and catalyst concentration lead to undesired saponification as well as a reduction in the relative amount of methanol in the reaction mixture. The circular nature of contour reveals lower interaction of catalyst amount and reaction temperature on POME yield[56].

Figure 4a
Surface plot: Yield Vs.temperature and catalyst amount

Figure 4b
Contour plot: Yield Vs. catalyst amount and temperature

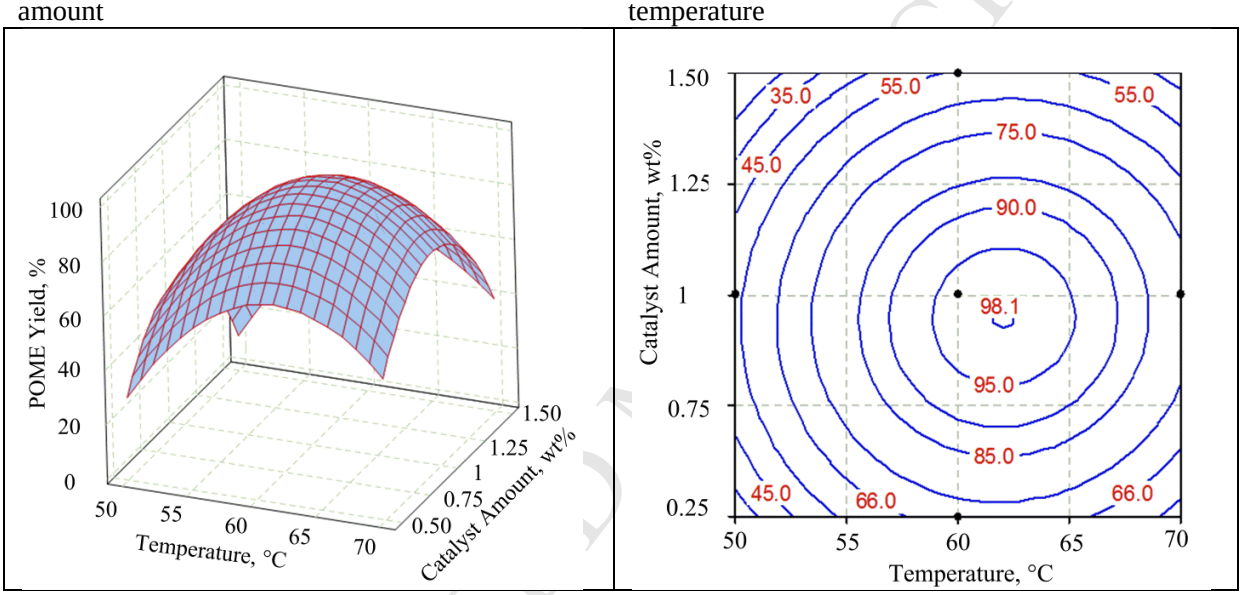


**Figure 4: Contour and surface plot of interaction of temperature and catalyst amount on POME yield**

**Figure 5a** and **5b** present the surface and contour plot for the interaction effect between reaction time ($X_3$) and temperature ($X_1$) toward POME yield. The molar ratio and catalyst amount were kept constant at 9:1 and 1wt% respectively. The yield increases with rising the temperature from a 50 °C to 60 °C for given reaction time. It is explained by the fact that the rise in temperature increases the possibility of microwave interaction as well as the generation of heat due to rapid dipole rotation[57]. At 50°C, extending the reaction time from 0.5 to 10.5 minutes improve the POME yield from 53% to 58%. On the other hand, at 70°C, it reduces from 90% to 66%. Hence, biodiesel yield is improved by a combination of short time with high temperature as well as high time with low temperature. The biodiesel content raise to

greater than 98% in the range of 60 to 65 °C and 1 to 5 minutes time interval. The time interval required for biodiesel conversion is low due to the initial stage of microwave radiation promoted thermal accumulation of reaction mixture[58].

Figure 5a
Surface plot: Yield Vs.temperature and time

Figure 5b
Contour plot: Yield Vs. temperature and time

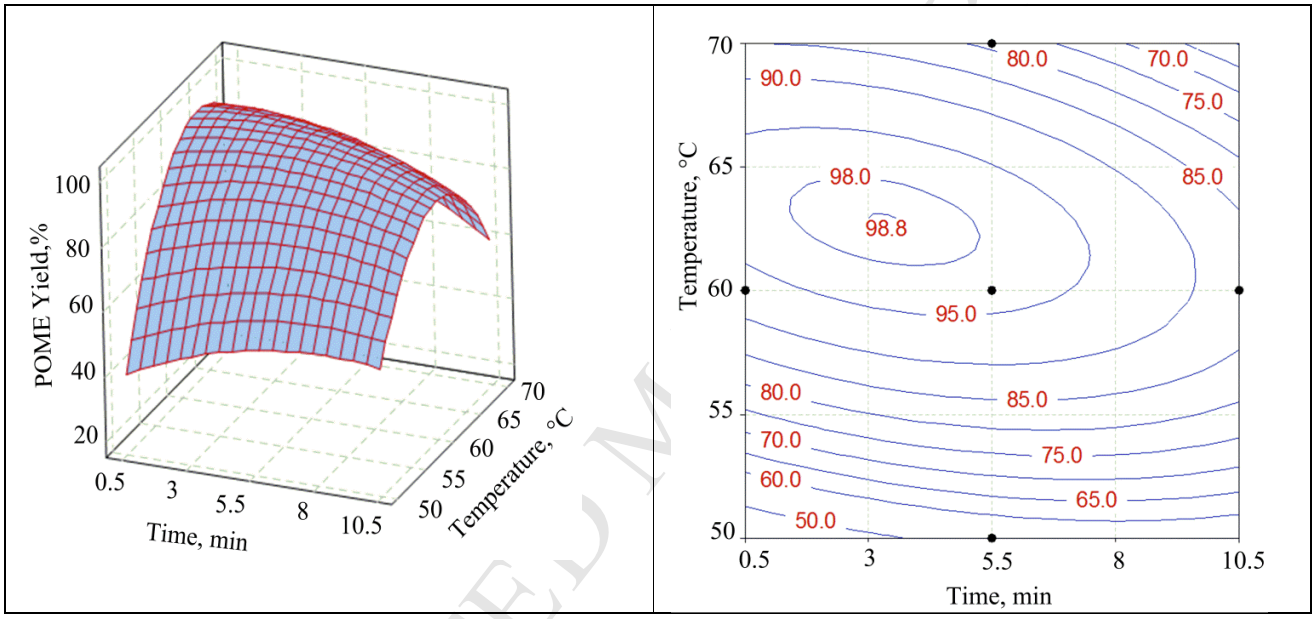


**Figure 5: Contour and surface plot showing interaction of temperature and time on POME yield**

Figure 6a and 6b exhibit the interaction of temperature($X_1$) and the molar ratio($X_4$) on POME yield. Similar nature of interaction plot was reported in the literature[59]. The poor yield obtained at the lower temperature and molar ratio of methanol to oil. At higher temperature, the yield significantly improved. Surprisingly yield reduced at elevated temperature (70°C), the probable reason was vaporization of methanol from the reaction flask. For all range of temperature under study, the rise in a molar ratio from 3:1 to 9:1 favored the forward reaction rate resulted in improvement in yield. At, the excess molar ratio of 15:1, the yield decreased mainly due to relative dilution of catalyst amount and lower microwave heat available for oil[60]. The observed yield was 99% at 10:1 methanol to oil molar ratio and 62°C temperature.

290

291

Figure 6a
Surface plot: Yield Vs. molar ratio and temperature

Figure 6b
Contour plot: Yield Vs. molar ratio and temperature

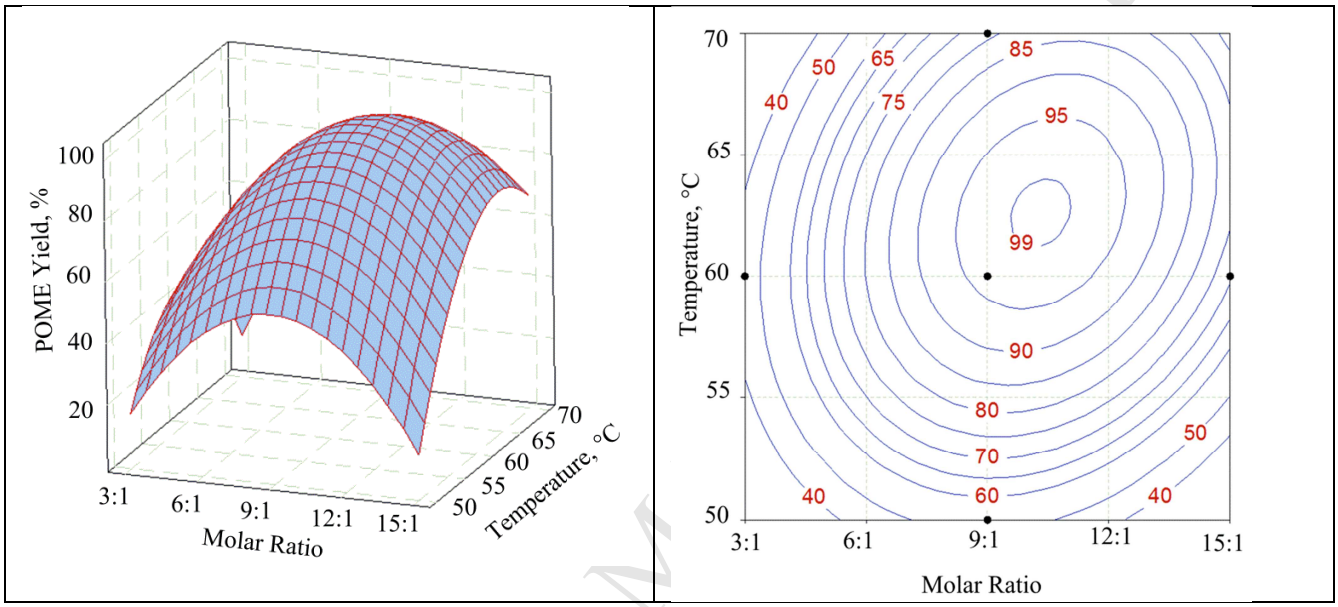


292 **Figure 6: Contour and surface plot of interaction of molar ratio and temperature on POME yield**

293 The simultaneous effect of the reaction time ($X_3$) and catalyst amount($X_2$) on yield are presented in the 3D
294 surface plot(**Figure 7a**), and contour plot(**Figure 7b**). At low catalyst loading, increasing the time from 0.5
295 to 10.5 minutes helps to improve the interaction of triglycerides with methanol and speed up the methyl
296 ester formation. Thus for low catalyst amount, rise in time enhances the yield. However, it is not true with
297 high catalytic loading as the excess catalyst initiate an undesired soap formation of fatty acid and
298 entrainment of biodiesel[61]. The substantial improvement in yield up to 96% obtained at 1±0.1% catalyst
299 concentration and 4±1 minute time interval.

300

301

302

Figure 7a
Surface plot: Yield Vs. catalyst amount and time

Figure 7b
Contour plot: Yield Vs.catalyst amount and time

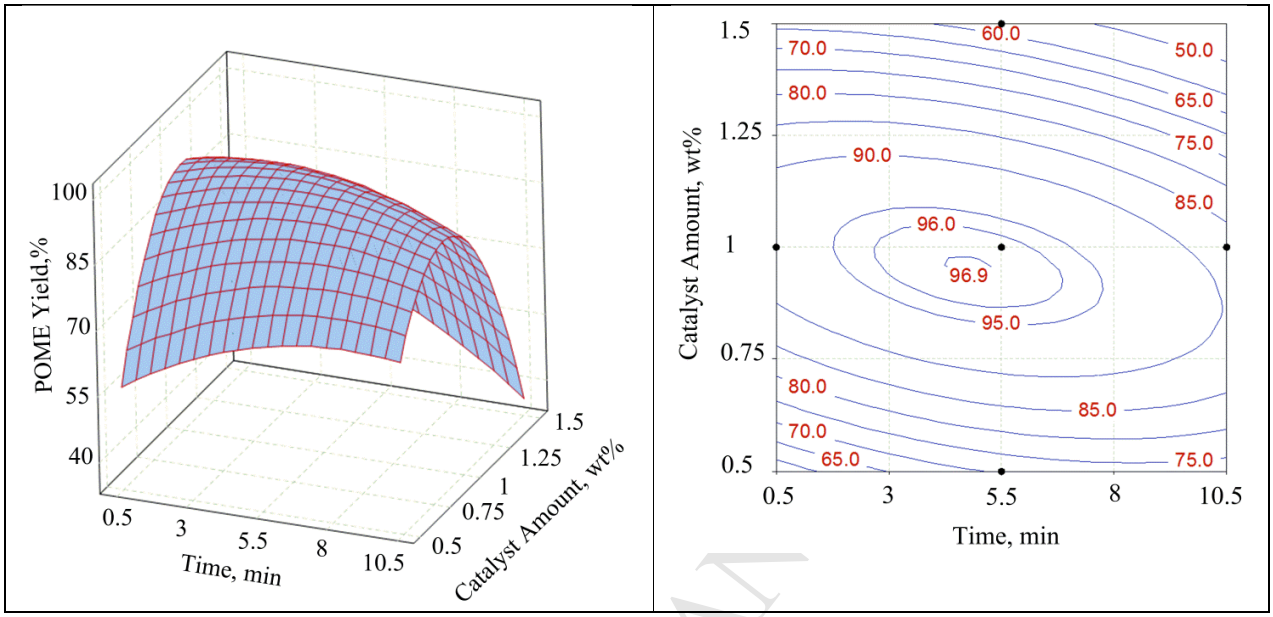


**Figure 7: Contour and surface plot of interaction of time and catalyst amount on POME yield**

**Figure 8a** and **8b** demonstrate a 3D surface and contour plot of the interaction of catalyst amount($X_2$) and molar ratio($X_4$) on POME yield. The poor yield obtained at the lower molar ratio and catalyst amount. It occurs due to consumption of methanol during the reaction, less catalyst amount and the possibility of a reversible reaction. The combined effect of high catalyst loading and the excess molar ratio lowers microwave heat available to triglyceride, increases the solubility of glycerol in biodiesel as well as increases possible side reaction. It resultes in a reduction of POME yield. At a lower molar ratio, the yield is increased from 20 % to up to 50%, when catalyst concentration increaing from 0.5 wt % to 1 wt%. Further increase in catalyst amount to 1.5 wt% reduces the yield up to 30%. It is occurred due to increase in solution viscosity and undesired saponification of free fatty acid. Similarly, at low catalyst concentration, increasing the molar ratio from 3:1 to 12:1 enlarges POME yield from 20 % to 78%. However, at an excess molar ratio of methanol to oil, relative dilution of catalyst adversely affects biodiesel yield. The similar pattern has been reported by Ngadi et al[62]. Based on the surface and contour plot, the combined effect of the molar ratio and catalyst amount leads to the increment in POME yield up to an optimum point.

318

Figure 8a
Surface plot: Yield Vs. catalyst amount and the molar ratio

Figure 8b
Contour plot: Yield Vs. catalyst amount and the molar ratio

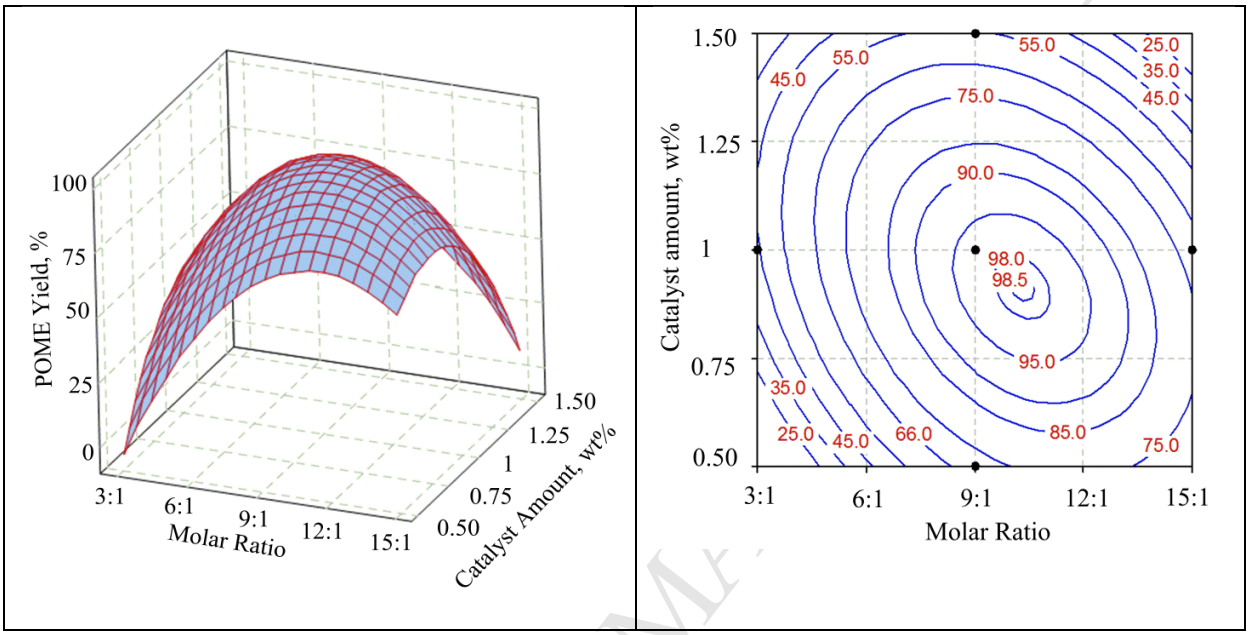


319 **Figure 8: Contour and surface plot of interaction of molar ratio and catalyst amount on POME yield**

320

321 Figure 9a and 9b present the simultaneous interaction of the molar ratio and reaction time on POME
322 yield. poor yield is observed at a 3:1 molar ratio and short reaction time. However, yield increases up to
323 97% at the moderate time and molar ratio. Further increment in molar ratio beyond 9:1 reduces POME
324 yield. It is due to increase in solubility of methanol in both phases and difficulty in separation. The
325 optimal molar ratio plays a vital role in improvement of the POME yield because a lower molar ratio
326 causes an incomplete reaction and the higher ratio decrease the yield. Similarly, for the rise in time above
327 optimum for all range of the molar ratio resulted in a decrease in the yield mainly due to possibilities of
328 backward reaction. It is in agreement with the results reported in the literature[61,63]

329

330

331

Figure 9a
Surface plot: Yield Vs. time and molar ratio

Figure 9b
Contour plot: Yield Vs. time and molar ratio

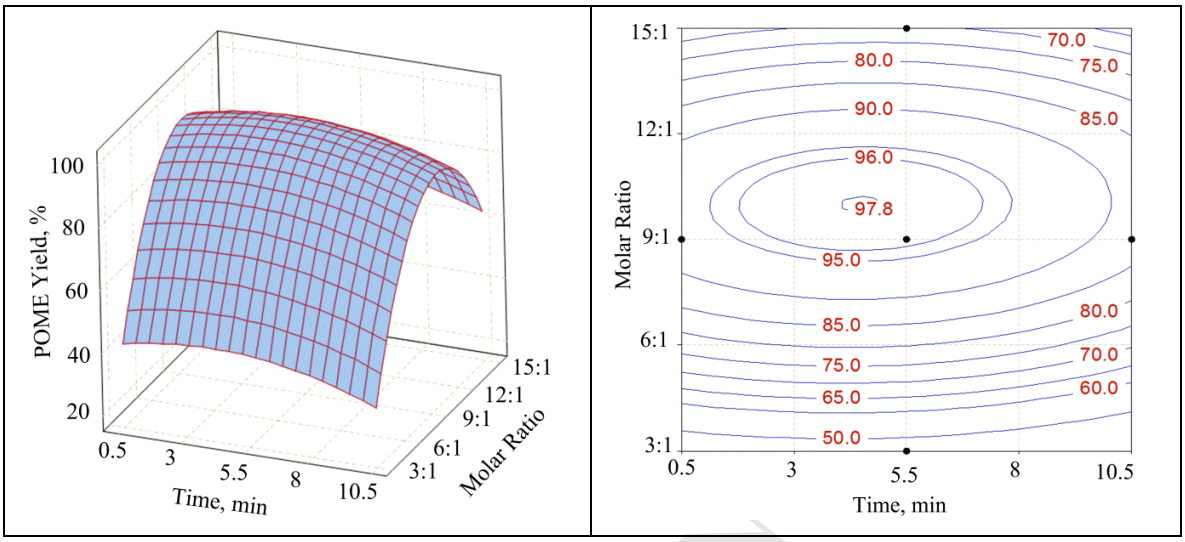


332 **Figure 9: Contour and surface plot of interaction of time and molar ratio on POME yield**

333

334 4.3 Optimization and validation

335 Optimization of the Process variable to maximize POME yield was performed using response surface
336 optimizer with the variable range under study. The maximum POME yield of 99.99% obtained under with
337 desirability of component 1(supplementary S2). The optimized values of temperature, catalyst, methanol
338 to oil molar ratio, and time were found to be 62.33°C, 0.95 wt%, 3.3 minute, and 9.5:01. These optimum
339 process parameters validated by triplication of experiments, at the optimal conditions (supplementary
340 S3). Thin layer chromatography (TLC) test was performed using silica gel fluorescent indicator F254.
341 The solvent hexane, diethyl ether, and acetic acid with volume ratio 80:20:1 was used for TLC. The spot
342 observed at retention factor (Rf) 0.67, 0.43 and 0.33 correspond to the position of methyl esters, Di-
343 glyceride, and mono-glyceride respectively (supplementary S4). No spot for triglyceride with Rf=0.56 in
344 the final product indicating close to complete conversion of Papaya oil into its methyl esters. Further the
345 optimized POME was analyzed using 1H NMR (supplementary S5). The absence of the peaks for

triglyceride protons at δ = 4.2–4.3 ppm and the presence of methyl resonance at δ=3.66 ppm confirmed the higher conversion of oil into biodiesel. The yield of biodiesel was calculated by Eq. (6)

$$\text{Yield} = 100 * \left(\frac{2*\text{AME}}{3*\text{A}\alpha\text{CH2}}\right) \qquad (6)$$

=100*(2*0.965)/3*(0.6466)

=99.4%

AME : Integration value of the protons of the methyl esters (the strong singlet peak)

Aα-$CH_2$ :Integration value of the methylene protons.

The experimentally observed mean yield of FAME (99.30 %) is in close agreement with the expected maximum yield(99.9%) suggested by the model equation.

Physicochemical properties of Microwave-assisted POME such as specific gravity, flash point, viscosity, cloud point, free fatty acid content, heating value, and cetane no were determined and summarized in **Table 6**. These physicochemical properties of produced biodiesel are in close agreement with the ASTM D6751.

Table 6

Physicochemical properties and characteristic of (POME) Papaya oil methyl ester

| Properties(unit) | Papaya oil methyl ester | ASTM D 6751-12 |
|---|---|---|
| Specific gravity($gcc^{-1}$) | 0.88 | 0.86-0.9 |
| Flash point(°C) | 135 | >130 |
| Viscosity at 40 °C (cSt) $mm^2s^{-1}$ | 3.68 | 1.9-6 |
| Molecular weight, g/mol | 276 | ---- |
| Cloud point (°C) | -0.1 | 5 |
| Free fatty acids% | <0.40 | <1.60 |
| Acid number (mg KOH g−1) | <0.20 | <0.80 |
| Heating value (calorific value) (MJ kg−1) | 38.50 | ----- |
| Cetane no. | 57.53 | 47 |

**Table 6: Physicochemical properties and characteristics of microwave-assisted POME**

## 5. Conclusions

Experimental investigation of microwave-assisted transesterification of Papaya oil was investigated using response surface methodology employing central composite design. The polynomial equation with $R^2$ = 0.9772 suggested that the RSM could predict the experimental results with high accuracy. The finding revealed that molar ration, temperature, and catalyst amount has a major influence on POME yield. The experimental finding suggested that microwave enhanced the conversion of oil into biodiesel. Close to 99% of yield obtained within a time interval of three minutes. Optimization of these process parameters, suggested 9.5:1 methanol to oil molar ratio, 0.95 wt% NaOH catalyst amount, 3.3 minutes time of reaction and 62.23°C temperature. The corresponding yield of 99.9% was in close agreement with experimental yield 99.3% at optimum condition. The key properties of POME were found to meet the biodiesel standards.

## References:


[1] A.V. Veličković, O.S. Stamenković, Z.B. Todorović, V.B. Veljković, Application of the full factorial design to optimization of base-catalyzed sunflower oil ethanolysis, Fuel. 104 (2013) 433–442. doi:http://dx.doi.org/10.1016/j.fuel.2012.08.015.

[2] A.W. Go, S. Sutanto, L.K. Ong, P.L. Tran-Nguyen, S. Ismadji, Y.-H. Ju, Developments in in-situ (trans) esterification for biodiesel production: A critical review, Renew. Sustain. Energy Rev. 60 (2016) 284–305. doi:http://dx.doi.org/10.1016/j.rser.2016.01.070.

[3] L. Gu, W. Huang, S. Tang, S. Tian, X. Zhang, A novel deep eutectic solvent for biodiesel preparation using a homogeneous base catalyst, Chem. Eng. J. 259 (2015) 647–652. doi:http://dx.doi.org/10.1016/j.cej.2014.08.026.

[4] Carlo Hamelinck, Michèle Koper, Mario Ragwitz, renewable energy progress and biofuels sustainability, (2014). https://ec.europa.eu/energy/sites/ener/files/documents/Final%20report%20-November%202014.pdf (accessed July 15, 2017).

[5] A.S. Reshad, D. Panjiara, P. Tiwari, V.V. Goud, Two-step process for production of methyl ester from rubber seed oil using barium hydroxide octahydrate catalyst: Process optimization, J. Clean. Prod. 142, Part 4 (2017) 3490–3499. doi:http://dx.doi.org/10.1016/j.jclepro.2016.10.118.

[6] P.D. Patil, H. Reddy, T. Muppaneni, S. Deng, Biodiesel fuel production from algal lipids using supercritical methyl acetate (glycerin-free) technology, Fuel. 195 (2017) 201–207. doi:http://dx.doi.org/10.1016/j.fuel.2016.12.060.

[7] N. Sootchiewcharn, L. Attanatho, P. Reubroycharoen, Biodiesel Production from Refined Palm Oil using Supercritical Ethyl Acetate in A Microreactor, Energy Procedia. 79 (2015) 697–703. doi:http://dx.doi.org/10.1016/j.egypro.2015.11.560.
[8] N.M. Niza, K.T. Tan, K.T. Lee, Z. Ahmad, Influence of impurities on biodiesel production from Jatropha curcas L. by supercritical methyl acetate process, J. Supercrit. Fluids. 79 (2013) 73–75. doi:http://dx.doi.org/10.1016/j.supflu.2013.02.021.
[9] D. Fabbri, V. Bevoni, M. Notari, F. Rivetti, Properties of a potential biofuel obtained from soybean oil by transmethylation with dimethyl carbonate, Fuel. 86 (2007) 690–697. doi:http://dx.doi.org/10.1016/j.fuel.2006.09.003.
[10] S. Righi, V. Bandini, D. Fabbri, M. Cordella, C. Stramigioli, A. Tugnoli, Modelling of an alternative process technology for biofuel production and assessment of its environmental impacts, J. Clean. Prod. 122 (2016) 42–51. doi:http://dx.doi.org/10.1016/j.jclepro.2016.02.047.
[11] A.K. Tiwari, A. Kumar, H. Raheman, Biodiesel production from jatropha oil (Jatropha curcas) with high free fatty acids: An optimized process, Biomass Bioenergy. 31 (2007) 569–575. doi:http://dx.doi.org/10.1016/j.biombioe.2007.03.003.
[12] A.A. Shankar, P.R. Pentapati, R.K. Prasad, Biodiesel synthesis from cottonseed oil using homogeneous alkali catalyst and using heterogeneous multi walled carbon nanotubes: Characterization and blending studies, Egypt. J. Pet. (2016). doi:http://dx.doi.org/10.1016/j.ejpe.2016.04.001.
[13] I.R. Sitepu, L.A. Garay, R. Sestric, D. Levin, D.E. Block, J.B. German, K.L. Boundy-Mills, Oleaginous yeasts for biodiesel: Current and future trends in biology and production, Biotechnol. Adv. 32 (2014) 1336–1360. doi:http://dx.doi.org/10.1016/j.biotechadv.2014.08.003.
[14] P. Verma, M.P. Sharma, Comparative analysis of effect of methanol and ethanol on Karanja biodiesel production and its optimisation, Fuel. 180 (2016) 164–174. doi:http://dx.doi.org/10.1016/j.fuel.2016.04.035.
[15] S.T.. S.A.. R.A.A.. E.S. El Sherbiny, Production of biodiesel using the microwave technique, J. Adv. Res. 1 (2010) 309–314. doi:10.1016/j.jare.2010.07.003.
[16] A. Arumugam, V. Ponnusami, Biodiesel production from Calophyllum inophyllum oil using lipase producing Rhizopus oryzae cells immobilized within reticulated foams, Renew. Energy. 64 (2014) 276–282. doi:http://dx.doi.org/10.1016/j.renene.2013.11.016.
[17] H.C. Ong, A.S. Silitonga, H.H. Masjuki, T.M.I. Mahlia, W.T. Chong, M.H. Boosroh, Production and comparative fuel properties of biodiesel from non-edible oils: Jatropha curcas, Sterculia foetida and Ceiba pentandra, Energy Convers. Manag. 73 (2013) 245–255. doi:http://dx.doi.org/10.1016/j.enconman.2013.04.011.
[18] M. Takase, T. Zhao, M. Zhang, Y. Chen, H. Liu, L. Yang, X. Wu, An expatiate review of neem, jatropha, rubber and karanja as multipurpose non-edible biodiesel resources and comparison of their fuel, engine and emission properties, Renew. Sustain. Energy Rev. 43 (2015) 495–520. doi:http://dx.doi.org/10.1016/j.rser.2014.11.049.
[19] V.V.. V.B.. G. Borugadda, Thermal, oxidative and low temperature properties of methyl esters prepared from oils of different fatty acids composition: A comparative study, Thermochim. Acta. 577 (2014) 33–40. doi:10.1016/j.tca.2013.12.008.
[20] V.V.. V.B.. G. Borugadda, Biodiesel production from renewable feedstocks: Status and opportunities, Renew. Sustain. Energy Rev. 16 (2012) 4763–4784. doi:10.1016/j.rser.2012.04.010.
[21] FAOSTAT, FAOSTAT, Http://Www.Fao.Org/Faostat/En/#data/QC. (2013). http://www.fao.org/faostat/en/#data/QC (accessed July 15, 2017).
[22] C. Reddy, All About Papaya in India, Papaya India. (2013). http://theindianvegan.blogspot.com/2013/03/all-about-papaya-in-india.html (accessed March 21, 2017).

[23] W.-J. Lee, M.-H. Lee, N.-W. Su, Characteristics of papaya seed oils obtained by extrusion–expelling processes, J. Sci. Food Agric. 91 (2011) 2348–2354. doi:10.1002/jsfa.4466.
[24] R. Naureen, M. Tariq, I. Yusoff, A.J.K. Chowdhury, M.A. Ashraf, Synthesis, spectroscopic and chromatographic studies of sunflower oil biodiesel using optimized base catalyzed methanolysis, Saudi J. Biol. Sci. 22 (2015) 332–339. doi:http://dx.doi.org/10.1016/j.sjbs.2014.11.017.
[25] M. Sánchez, F. Bergamin, E. Peña, M. Martínez, J. Aracil, A comparative study of the production of esters from Jatropha oil using different short-chain alcohols: Optimization and characterization, Fuel. 143 (2015) 183–188. doi:http://dx.doi.org/10.1016/j.fuel.2014.11.064.
[26] P. Thliveros, E.U. Kiran, C. Webb, Microbial biodiesel production by direct methanolysis of oleaginous biomass, Bioresour. Technol. 157 (2014) 181–187. doi:http://dx.doi.org/10.1016/j.biortech.2014.01.111.
[27] Q. Wang, C. Yao, Z. Dou, B. Wang, T. Wu, Effect of intake pre-heating and injection timing on combustion and emission characteristics of a methanol fumigated diesel engine at part load, Fuel. 159 (2015) 796–802. doi:http://dx.doi.org/10.1016/j.fuel.2015.07.032.
[28] C. Domingues, M.J.N. Correia, R. Carvalho, C. Henriques, J. Bordado, A.P.S. Dias, Vanadium phosphate catalysts for biodiesel production from acid industrial by-products, J. Biotechnol. 164 (2013) 433–440. doi:http://dx.doi.org/10.1016/j.jbiotec.2012.07.009.
[29] A.C.C. Bacilla, M.R. de Freitas, A. Bail, V.C. dos Santos, N. Nagata, Â. Silva, L. Marçal, K.J. Ciuffi, S. Nakagaki, Heterogeneous/homogeneous esterification reaction catalyzed by a solid based on a vanadium salt, J. Mol. Catal. Chem. 422 (2016) 221–233. doi:http://dx.doi.org/10.1016/j.molcata.2015.12.018.
[30] J. Mukherjee, M.N. Gupta, Dual bioimprinting of Thermomyces lanuginosus lipase for synthesis of biodiesel, Biotechnol. Rep. 10 (2016) 38–43. doi:http://dx.doi.org/10.1016/j.btre.2016.02.005.
[31] S. Jazzar, P. Olivares-Carrillo, A.P. de los Ríos, M.N. Marzouki, F.G. Acién-Fernández, J.M. Fernández-Sevilla, E. Molina-Grima, I. Smaali, J. Quesada-Medina, Direct supercritical methanolysis of wet and dry unwashed marine microalgae (Nannochloropsis gaditana) to biodiesel, Appl. Energy. 148 (2015) 210–219. doi:http://dx.doi.org/10.1016/j.apenergy.2015.03.069.
[32] G.T. Ang, S.N. Ooi, K.T. Tan, K.T. Lee, A.R. Mohamed, Optimization and kinetic studies of sea mango (Cerbera odollam) oil for biodiesel production via supercritical reaction, Energy Convers. Manag. 99 (2015) 242–251. doi:http://dx.doi.org/10.1016/j.enconman.2015.04.037.
[33] S. Lim, S.S. Hoong, L.K. Teong, S. Bhatia, Supercritical fluid reactive extraction of Jatropha curcas L. seeds with methanol: A novel biodiesel production method, Bioresour. Technol. 101 (2010) 7169–7172. doi:http://dx.doi.org/10.1016/j.biortech.2010.03.134.
[34] P.E.. R.B.. P.T.. S. Levine, Biodiesel production from wet algal biomass through in situ lipid hydrolysis and supercritical transesterification, Energy Fuels. 24 (2010) 5235–5243. doi:10.1021/ef1008314.
[35] C. Román-Figueroa, P. Olivares-Carrillo, M. Paneque, F.J. Palacios-Nereo, J. Quesada-Medina, High-yield production of biodiesel by non-catalytic supercritical methanol transesterification of crude castor oil (Ricinus communis), Energy. 107 (2016) 165–171. doi:http://dx.doi.org/10.1016/j.energy.2016.03.136.
[36] W.W.S. Ho, H.K. Ng, S. Gan, W.L. Chan, Ultrasound-assisted transesterification of refined and crude palm oils using heterogeneous palm oil mill fly ash supported calcium oxide catalyst, Energy Sci. Eng. 3 (2015) 257–269. doi:10.1002/ese3.56.
[37] Y. Xiang, L. Wang, Y. Jiao, Ultrasound strengthened biodiesel production from waste cooking oil using modified coal fly ash as catalyst, J. Environ. Chem. Eng. 4 (2016) 818–824. doi:http://dx.doi.org/10.1016/j.jece.2015.12.031.

[38] N. Gharat, V.K. Rathod, Ultrasound assisted enzyme catalyzed transesterification of waste cooking oil with dimethyl carbonate, Ultrason. Sonochem. 20 (2013) 900–905. doi:http://dx.doi.org/10.1016/j.ultsonch.2012.10.011.
[39] A.S. Badday, A.Z. Abdullah, K.-T. Lee, Transesterification of crude Jatropha oil by activated carbon-supported heteropolyacid catalyst in an ultrasound-assisted reactor system, Renew. Energy. 62 (2014) 10–17. doi:http://dx.doi.org/10.1016/j.renene.2013.06.037.
[40] O.. N.. Y. Azcan, Microwave assisted transesterification of waste frying oil and concentrate methyl ester content of biodiesel by molecular distillation, Fuel. 104 (2013) 614–619. doi:10.1016/j.fuel.2012.06.084.
[41] Y.-C. Lin, S.-C. Chen, C.-E. Chen, P.-M. Yang, S.-R. Jhang, Rapid Jatropha-biodiesel production assisted by a microwave system and a sodium amide catalyst, Fuel. 135 (2014) 435–442. doi:http://dx.doi.org/10.1016/j.fuel.2014.07.023.
[42] R. Priambodo, T.-C. Chen, M.-C. Lu, A. Gedanken, J.-D. Liao, Y.-H. Huang, Novel Technology for Bio-diesel Production from Cooking and Waste Cooking Oil by Microwave Irradiation, Energy Procedia. 75 (2015) 84–91. doi:http://dx.doi.org/10.1016/j.egypro.2015.07.143.
[43] V.L. Gole, P.R. Gogate, Intensification of synthesis of biodiesel from non-edible oil using sequential combination of microwave and ultrasound, Fuel Process. Technol. 106 (2013) 62–69. doi:10.1016/j.fuproc.2012.06.021.
[44] A.. N.. D. Azcan, Microwave assisted transesterification of rapeseed oil, Fuel. 87 (2008) 1781–1788. doi:10.1016/j.fuel.2007.12.004.
[45] F.O.A. Tolulope A. Adewole, Methanolysis of Carica papaya Seed Oil for Production of Biodiesel, Hindwai. 2014 (2014) 6 pages. doi:10.1155/2014/904076.
[46] L.F. Chuah, J.J. Klemeš, S. Yusup, A. Bokhari, M.M. Akbar, A review of cleaner intensification technologies in biodiesel production, J. Clean. Prod. (2016). doi:http://dx.doi.org/10.1016/j.jclepro.2016.05.017.
[47] P.D. Muley, D. Boldor, Investigation of microwave dielectric properties of biodiesel components, Bioresour. Technol. 127 (2013) 165–174. doi:http://dx.doi.org/10.1016/j.biortech.2012.10.008.
[48] Maria, Alovert, Andrew M, The 3-27 Conversion Test | Quality Testing, (2017). http://www.make-biodiesel.org/Quality-Testing/the-3-27-conversion-test.html (accessed November 2, 2017).
[49] H. Jaliliannosrati, N.A.S. Amin, A. Talebian-Kiakalaieh, I. Noshadi, Microwave assisted biodiesel production from Jatropha curcas L. seed by two-step in situ process: Optimization using response surface methodology, Bioresour. Technol. 136 (2013) 565–573. doi:http://dx.doi.org/10.1016/j.biortech.2013.02.078.
[50] A.S. Badday, A.Z. Abdullah, K.-T. Lee, Optimization of biodiesel production process from Jatropha oil using supported heteropolyacid catalyst and assisted by ultrasonic energy, Renew. Energy. 50 (2013) 427–432. doi:http://dx.doi.org/10.1016/j.renene.2012.07.013.
[51] M. Barekati-Goudarzi, D. Boldor, D.B. Nde, In-situ transesterification of seeds of invasive Chinese tallow trees (Triadica sebifera L.) in a microwave batch system (GREEN3) using hexane as co-solvent: Biodiesel production and process optimization, Bioresour. Technol. 201 (2016) 97–104. doi:http://dx.doi.org/10.1016/j.biortech.2015.11.028.
[52] P.D. Patil, V.G. Gude, L.M. Camacho, S. Deng, Microwave-Assisted Catalytic Transesterification of Camelina Sativa Oil, Energy Fuels. 24 (2010) 1298–1304. doi:10.1021/ef9010065.
[53] M.-C. Hsiao, C.-C. Lin, Y.-H. Chang, Microwave irradiation-assisted transesterification of soybean oil to biodiesel catalyzed by nanopowder calcium oxide, Fuel. 90 (2011) 1963–1967. doi:http://dx.doi.org/10.1016/j.fuel.2011.01.004.
[54] A.K. Sharma, P.K. Sahoo, S. Singhal, G. Joshi, Exploration of upstream and downstream process for microwave assisted sustainable biodiesel production from microalgae Chlorella vulgaris, Bioresour. Technol. 216 (2016) 793–800. doi:10.1016/j.biortech.2016.06.013.

[55] X. Wu, D.Y.C. Leung, Optimization of biodiesel production from camelina oil using orthogonal experiment, Appl. Energy. 88 (2011) 3615–3624. doi:10.1016/j.apenergy.2011.04.041.
[56] X. Yuan, J. Liu, G. Zeng, J. Shi, J. Tong, G. Huang, Optimization of conversion of waste rapeseed oil with high FFA to biodiesel using response surface methodology, Renew. Energy. 33 (2008) 1678–1684. doi:10.1016/j.renene.2007.09.007.
[57] I.K. Hong, H. Jeon, H. Kim, S.B. Lee, Preparation of waste cooking oil based biodiesel using microwave irradiation energy, J. Ind. Eng. Chem. 42 (2016) 107–112. doi:10.1016/j.jiec.2016.07.035.
[58] J. Pullen, K. Saeed, Investigation of the factors affecting the progress of base-catalyzed transesterification of rapeseed oil to biodiesel FAME, Fuel Process. Technol. 130 (2015) 127–135. doi:10.1016/j.fuproc.2014.09.013.
[59] I. Sengo, J. Gominho, L. d'Orey, M. Martins, E. d'Almeida-Duarte, H. Pereira, S. Ferreira-Dias, Response surface modeling and optimization of biodiesel production from Cynara cardunculus oil, Eur. J. Lipid Sci. Technol. (2010) NA-NA. doi:10.1002/ejlt.200900135.
[60] P. Khemthong, C. Luadthong, W. Nualpaeng, P. Changsuwan, P. Tongprem, N. Viriya-empikul, K. Faungnawakij, Industrial eggshell wastes as the heterogeneous catalysts for microwave-assisted biodiesel production, Catal. Today. 190 (2012) 112–116. doi:10.1016/j.cattod.2011.12.024.
[61] S. Dharma, H.H. Masjuki, H.C. Ong, A.H. Sebayang, A.S. Silitonga, F. Kusumo, T.M.I. Mahlia, Optimization of biodiesel production process for mixed Jatropha curcas–Ceiba pentandra biodiesel using response surface methodology, Energy Convers. Manag. 115 (2016) 178–190. doi:10.1016/j.enconman.2016.02.034.
[62] M. Mohamad, N. Ngadi, S.L. Wong, M. Jusoh, N.Y. Yahya, Prediction of biodiesel yield during transesterification process using response surface methodology, Fuel. 190 (2017) 104–112. doi:10.1016/j.fuel.2016.10.123.
[63] C.S. Latchubugata, R.V. Kondapaneni, K.K. Patluri, U. Virendra, S. Vedantam, Kinetics and optimization studies using Response Surface Methodology in biodiesel production using heterogeneous catalyst, Chem. Eng. Res. Des. 135 (2018) 129–139. doi:10.1016/j.cherd.2018.05.022.

Highlights

- Unexplored and nonedible Papaya seed oil investigated for biodiesel synthesis.
- Microwave-assisted transesterification of Papaya oil into its methyl ester was explored.
- Optimization of four process variables was studied by using response surface methodology.
- Close to 99% yield of biodiesel obtained at 62.33 °C, 0.95 wt% alkali catalysts, 3.30 minutes, and 9.50:1 methanol to oil molar ratio.